Journal of Cell Science 104,843-852 (1993)
Printed in Great Britain © The Company of Biologists Limited 1993

Different patterns of rDNA distribution in *Pisum sativum* nucleoli correlate with different levels of nucleolar activity

Martin I. Highett, David J. Rawlins and Peter J. Shaw*

Department of Cell Biology, John Innes Centre, Colney Lane, Norwich NR4 7UH, UK

*Author for correspondence

SUMMARY

We have used in situ hybridization with probes to rDNA, labelled either with digoxygenin or directly with fluorescein, to determine the arrangement of these genes within the nucleoli of *Pisum sativum* L. root cells. Confocal laser scanning microscopy was used to image the three-dimensional structures revealed, but we have also compared this technique with deconvolution of conventional (wide-field) fluorescence images measured with a cooled CCD camera, and have shown that the results are remarkably similar. When the deconvolution technique was applied to the confocal data it gave clearer images than could be achieved by confocal microscopy alone. We have analysed the distribution of rDNA in the different cell types observable in root tips: the quiescent centre; active meristematic cells; and relatively differentiated root cap, epidermal and cortical cells. In addition to four perinucleolar knobs of condensed, inactive rDNA genes, corresponding to the four nucleolar organizers in *P. sativum*, which were the most brightly labelled structures, several characteristic patterns of intranucleolar labelling were apparent, including bright foci, large central chromatin masses, and fine, decondensed interconnecting fibres. The larger and more active the nucleolus, the smaller the proportion of condensed perinucleolar rDNA. In some large and active meristematic nucleoli, all the internal rDNA is decondensed, showing that transcription cannot be restricted to the bright foci, and is most likely to occur on the decondensed fibres.

Key words: rDNA, confocal microscopy, gene transcription, 3-D structure, in situ hybridization

INTRODUCTION

It is well established that the nucleolus is the site of transcription of the rRNA genes, of the post-transcriptional processing of the RNA, and of its assembly into pre-ribosomal particles, along with the 5 S rRNA (transcribed outside the nucleolus and imported into it), and the various ribosomal proteins, imported from the cytoplasm. The nucleolus therefore provides a spatially defined system for the study of many important nuclear activities, including transcription, transcript processing, RNA and protein import, and pre-ribosomal subunit export (for reviews see Goessens, 1984; Hadjiolov, 1985; Warner, 1989).

In view of this, it is surprising that there is still so much uncertainty surrounding even the arrangement within the nucleolus of the rDNA (Jordan, 1991; Schwarzacher and Wachtler, 1991; Medina, 1989). Conventional thin-section electron microscopy shows three types of structure within nucleoli (Jordan, 1984): (1) lightly staining regions, typically approximately 0.2 μm in diameter but sometimes much larger, which have been termed fibrillar centres; (2) much more densely staining regions surrounding and extending from the fibrillar centres, termed dense fibrillar component; and (3) regions containing more or less densely packed granules, the granular component. Several studies have shown incorporated ^{3}H-labelled precursors in nascent trancripts to be located initially at the dense fibrillar component (Geuskens and Bernhard, 1966; Goessens, 1976; Hernandez-Verdun and Bouteille, 1979; Mirre and Stahl, 1978; Stahl, 1982; Deltour and Mosen, 1987), whereas Scheer and Rose (1984) used EM immunogold cytochemistry to show the presence of RNA polymerase I in the fibrillar centres. Although the localization of the polymerase cannot prove that it is active at these sites, this observation has led to the suggestion that all the active rDNA is located in the fibrillar centres. Thiry et al. (1988a,b) have demonstrated by in situ labelling at the EM level that the fibrillar centres in the nucleoli of Ehrlich tumour cells contain rDNA. In contrast to this, Wachtler et al. (1989) have shown labelling of the rDNA in the dense fibrillar component of human Sertoli cells, and little or no rDNA in the large single fibrillar centre of these cells. In onion cells, Martin et al. (1989) have shown labelling using an anti-DNA antibody in both the fibrillar centres and at least part of the surrounding dense fibrillar component. Thus there is little agreement on the location of the rDNA, if indeed its location is consistently related to observable EM ultrastructure, still less about where transcription may be taking place. Dif-

ferent models have placed transcription in each of the EM structural components, or even at the interface between fibrillar centre and dense fibrillar component (Jordan, 1991).

However, there may be significant problems with using EM post-section immunogold techniques for this type of study. It is difficult to obtain an accurate picture of the entire three-dimensional structure of a nucleolus by EM section analysis, as only a small proportion of any DNA present will be sufficiently exposed at the surface of a resin section for in situ labelling, substantially reducing the sensitivity of this type of labelling, and only very few cells are surveyed by EM techniques. In contrast, recent advances in optical microscopy coupled with fluorescence in situ hybridization enable us to overcome many of these problems. Fluorescence in situ hybridization has excellent specificity and sensitivity, and optical focal sectioning, using either confocal or conventional (wide-field) microscopy and image processing, provides good three-dimensional images of sub-cellular structures, and large areas of intact tissue can rapidly be surveyed. We have previously used in situ hybridization with double-stranded biotinylated DNA probes to show that in *Pisum sativum* there are four perinucleolar 'knobs' of condensed rDNA, corresponding to transcriptionally inactive portions of each of the four nucleolar organizers (NORs) of this species, as well as a number of internal foci of labelling, which we suggested may correspond to fibrillar centres (Rawlins and Shaw, 1990). More recently, we used the DNA stain DAPI (2,4-diamidino phenyl indole) to image the nucleolar DNA within both human MRC5 culture cells and *Spirogyra grevelliana* nucleoli (Jordan et al., 1992). Image measurement using wide-field epifluorescence microscopy with a sensitive, cooled CCD camera followed by data deconvolution showed that the distribution of DNA was more widespread than could be accounted for by location in the fibrillar centres alone. In the present paper we have used single-stranded RNA probes to the rDNA, which markedly increases the sensitivity and specificity of labelling, to reveal the detailed structure of the rDNA in various cell types present in the tissue. We also show that data deconvolution can be applied to confocal three-dimensional data to give clearer images than either confocal microscopy alone or deconvolution of wide-field CCD data.

MATERIALS AND METHODS

Specimen preparation

Seeds of *Pisum sativum* L. (cultivar Greenshaft JI430) were imbibed in aerated water for 12 hours, then germinated at 18ºC for 2 days on water-soaked paper towels. The terminal 3-5 mm of the radical were excised, under water, and fixed in 4% (w/v) formaldehyde/0.1% (v/v) glutaraldehyde in buffer (50 mM PIPES/KOH (pH 6.9), 5 mM EGTA, 5 mM $MgSO_4$) for 1 hour at room temperature. After washing 3 times in TBS (TBS: 25 mM Tris/HCl (pH 7.4), 140 mM NaCl, 3 mM KCl), 30-40 µm vibratome sections were cut under water and dried down on to glutaraldehyde-activated organosilane γ-aminoproyltriethoxy silane (APES)-coated multiwell slides. Slides were then stored at −20°C or used immediately. Tissue sections were treated four times for 15 minutes at room temperature with freshly prepared sodium borohydride solutions (1 mg/ml in PBS) (PBS: 140 mM NaCl, 3 mM KCl, 4 mM Na_2HPO_4, 2mM KH_2PO_4, pH 8.0) to reduce autofluorescence caused by glutaraldehyde. Sections were permeabilized with 2% (w/v) cellulase (Onozuka R-10) in TBS for 1 hour at room temperature.

Nucleic acid blotting

Digests were run out on 1.2% (w/v) agarose gels using standard conditions (Sambrook et al., 1989), and transferred to Hybond-N filters (Amersham) for filter hybridization experiments. After hybridization with digoxygenin-labelled probe and washing, the probe was detected with alkaline phosphatase-conjugated anti-digoxygenin (Boehringer), developed with nitro blue tetrazolium chloride and 5-bromo,4-chloro,3-indolyl phosphate (NBT/BCIP - Promega), used according to the manufacturer's instructions.

Preparation of probes

A single 9 kb rDNA repeat from *P. sativum* was sub-cloned into the Bluescript SK^+ vector (Stratagene) at the *Xba*I site. (The original clone, cDB1.07, was a gift from Dr J. Gatehouse, Department of Botany, University of Durham, Durham, UK.) Single-stranded RNA probes were generated as 'run-around' transcripts from the phage T7 promoter. The insert was oriented such that T7 polymerase produced sense RNA (complementary to the transcribed strand of the DNA). Label was incorporated into the probes by including either digoxigenin-11-UTP (Boehringer) or, more recently, fluorescein-12-UTP (Boehringer) in the in vitro transcription reaction. In order to improve penetration into the specimen the probe size was reduced to approximately 200 bases by a mild hydrolysis with carbonate (Cox et al., 1984).

In order to be sure that the probe used contained transcribed RNA from the entire length of the 9 kb rDNA insert, we probed blots of restriction digests of the Bluescript vector containing the insert. The probe hybridized to all the expected bands derived from the insert, showing that the in vitro transcription proceeded through the entire insert. Since there was also slight labelling of the plasmid band, we used an excess of unlabelled RNA transcribed from the plasmid alone or an unrelated insert to block non-specific binding in the in situ experiments.

In situ hybridization

Prior to hybridization single-stranded DNA target was produced by heat-denaturing the tissue sections for 5 min at 98°C in 0.1 × SSC (SSC: 150 mM NaCl, 15 mM sodium citrate) and then placing the slides in ice-cold 0.1 × SSC to prevent reannealing. A probe solution containing 0.5 µl digoxygenin- or fluorescein-labelled RNA (~200 ng/µl), 0.5 µl unlabelled RNA (~1000 ng/µl), 5 µl deionized formamide, 2 µl 50% dextran sulphate, 1 µl buffer (100 mM PIPES, pH 8.0, 10 mM EDTA), and 1 µl 3 M NaCl was added to each section. Slides were then placed in a damp chamber and incubated overnight at 37°C. Slides were then washed three times in 2 × SSC for 10 min, and finally in TBS for 3 min.

In the cases where fluorescein-labelled probe was used, no further reactions were used for probe detection. In order to detect digoxygenin-labelled probe, the specimens were incubated at 37°C for 45 min with 12.5 µl primary antibody (FITC-conjugated sheep anti-digoxygenin (Boehringer), diluted 1:100 in TBS containing 3% BSA and 0.02% sodium azide). They were then washed 3 times in TBS for 10 min. A second incubation followed at 37°C for 45 min with 12.5 µl secondary antibody (FITC-conjugated rabbit anti-sheep immunoglobulin - DAKO, diluted 1:100 in TBS containing 3% BSA and 0.02% sodium azide). The slides were finally washed again, counterstained with DAPI, and mounted in glycerol-based anti-fade solution (Citifluor).

In some control experiments the in situ labelling was preceded by either DNase or RNase digestion. For DNase digestion, the

sections were incubated at 37ºC for 60 min in a solution of RNase-free DNase I (1000 units/ml - Pharmacia) followed by 3 washes in a × 0.1 SSC solution to remove DNA fragments. For RNase digestion, the sections were incubated at 37ºC for 40 min in a solution of RNase A (7.5 units/ml - Sigma; treated at 90ºC for 10 min to remove DNase activity) followed by 3 washes in 0.1 × SSC solution to remove RNA fragments.

Microscopy

Confocal optical sections stacks were collected using a Biorad Lasersharp MRC-500 confocal scanning head mounted on a Zeiss Universal microscope as described previously (Rawlins and Shaw, 1990). Wide-field optical sections were collected using a charge-coupled device (CCD) camera (Photometrics Inc.) mounted on a Zeiss Universal microscope using the Leitz Planapo ×63/1.4 NA objective as described by Traas et al. (1992). Image deconvolution was carried out with the 3-D iterative constrained Jannson-van Cittert method using the program DECON3D written by Dr David Agard, and described by Agard et al. (1989), implemented on Titan computer. Measured point spread functions for either wide-field optics or confocal optics with the relevant detector pinhole size were used for the deconvolutions (Shaw and Rawlins, 1991a,b).

Montages of images were produced for display and interpretation of the various data sets. Alternatively, series of projections were calculated at different angles (Agard et al., 1989) and displayed as stereo pairs or sequentially to give the impression of rotation. In the calculation of projections, either the mean or the maximum intensity along each site line was used, usually the latter. Images were photographed directly from the monitor.

RESULTS

Characterization of in situ labelling targets

We have shown previously that the preservation of nuclear and cellular structure under the fixation conditions used was good (Rawlins and Shaw, 1990). We have also carried out electron microscopy of ultrathin sections of tissue fixed in this way, both before and after subjecting the sample to the in situ labelling procedures, and have shown that preservation of the nuclear contents is relatively good even at the electron microcope level of resolution. In order to be certain of the targets of hybridization in the tissue, we carried out a series of control experiments. In the absence of heat denaturation sense probe showed no labelling. Thus heat denaturation was absolutely necessary to produce single-stranded DNA target for probe hybridization. Pre-treatment of the specimens with RNase-free DNase removed all DNA target (as judged by DAPI labelling) and resulted in no labelling, whereas pre-treatment with DNase-free RNase had little or no effect. The result of this experiment is shown in Fig. 1. Other control experiments using labelled transcript from a plasmid containing no insert or using unlabelled anti-sense 5 S probe showed no labelling. Therefore all the labelling with the rDNA sense probe must be attributed to hybridization to endogenous rDNA.

Comparison of wide-field and confocal images

In a number of experiments we collected 3-D data sets of the same cell twice, once using confocal microscopy and once using conventional fluorescence optics with a low light level, cooled CCD camera. Each data set was then processed using the iterative, constrained deconvolution method, in each case using the appropriate measured point spread function (Shaw and Rawlins, 1991a; Agard et al., 1989). A single equivalent section from each of the four data sets from one such experiment is shown in Fig. 2. The most important conclusion from this was that deblurred, wide-field data are very similar to the unprocessed confocal data, although the former shows greater clarity and definition. The remarkable agreement between the two (Fig. 2b,c), even down to the finest image details, gives us confidence in the fidelity of both methods, and in the reliabil-

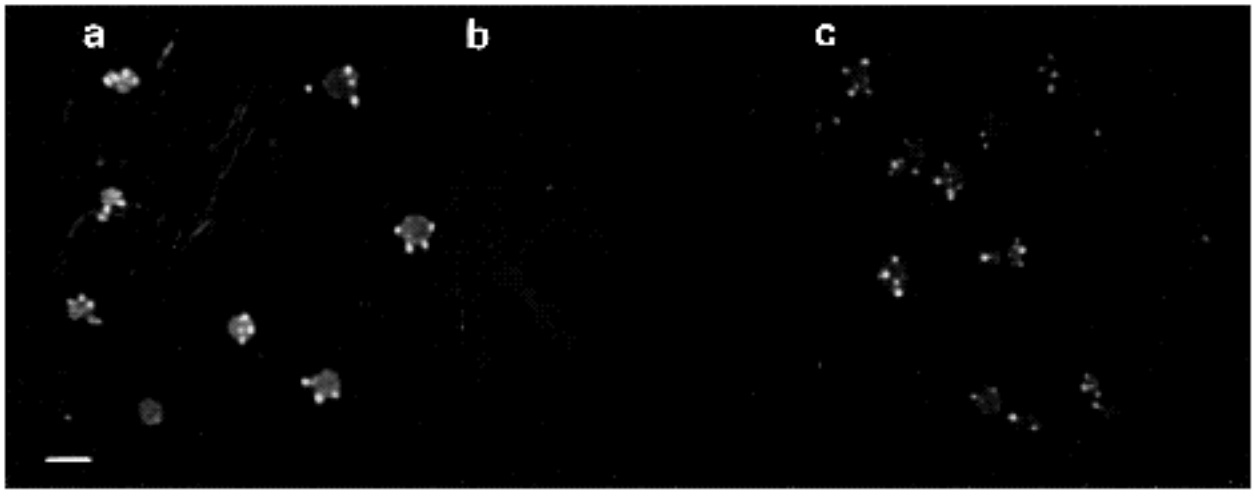

Fig. 1. Nuclease digestion control experiments. In each panel a projection of confocal sections covering a total depth of field of approximately 40 μm is shown. (a) A field of tissue probed with sense rDNA fluorescein-labelled probe after standard treatment. The perinucleolar knobs are brightly labelled, and some internal nucleolar labelling is apparent. The nuclear and cytoplasmic background is very low. (b) A similar field of tissue, pre-digested with RNase-free DNase, before in situ labelling. All labelling is lost. (c) A similar field of tissue, predigested with DNase-free RNase before in situ labelling. Both the internal labelling and the perinucleolar knobs are largely unaffected by RNase digestion. Bar, 10 μm.

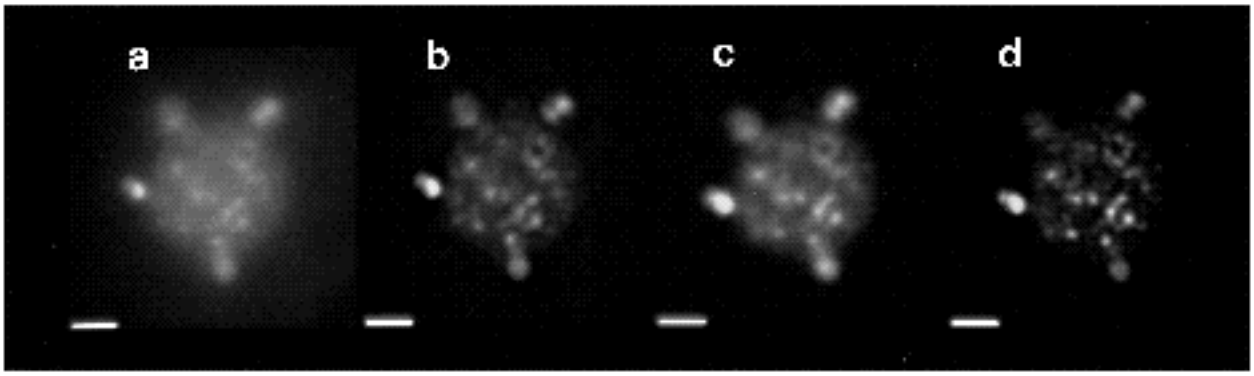

Fig. 2. Comparison of wide-field, confocal and deconvoluted data. (a) A single optical section, taken from a 3-D data stack, measured with wide-field fluorescence optics and a cooled CCD camera, from an in situ labelled nucleolus. (b) The same section taken from the 3-D data stack after deconvolution. The out-of-focus flare has been removed and the fine detail is revealed much more clearly. (c) An equivalent section from a 3-D data stack subsequently recorded from the same nucleolus using a confocal microscope. The agreement with the deconvoluted wide-field data is remarkably good, and extends to the finest details. (d) The same section taken from the confocal data stack after deconvolution using the confocal point spread function. The fine detail is revealed more clearly than in b or c. Bar, 2 μm.

ity with which we can interpret the image reconstructions produced. As we have previously shown, image deconvolution can equally well be applied to confocal data, using the appropriate measured confocal point spread function. The equivalent section from the deconvolved confocal data is shown in Fig. 2d. This data set gives the greatest clarity of all the four data sets, and thus all subsequent reconstructions were derived by deconvolution of confocal data. In most cases, the internal nucleolar rDNA structure is complicated and extensive. We found that a great deal of this detail is lost in stereo projections of the entire nucleolus; therefore we have shown stereo projections of limited slices through the centre or top of nucleoli. In each case the slice projections derive from 5 confocal optical sections, giving a depth of field of 1-2 μm.

Arrangement of rDNA within root cell nucleoli

Fig. 3 shows a low magnification confocal projection from a typical in situ hybridized tissue slice, and demonstrates that all the nucleoli in the slice are accessible to the probe, and that the labelling is highly specific to the nucleoli with very low background staining. We obtained equivalent results with either digoxygenin-labelled probes or probes directly labelled by incorporation of fluorescein-UTP. Most of the images shown in this paper were obtained using the fluorescein-labelled probes. The majority of root cells contained a single nucleolus. *P. sativum* has 2 pairs of nucleolar organizer chromosomes (chromosomes 4 and 7), and, as we have demonstrated before (Rawlins and Shaw, 1990), portions of these organizer regions remain outside the body of the nucleolus as perinucleolar knobs. The knobs were the most brightly labelled structures, and deconvoluted confocal images often showed considerable substructure within them, consistent with closely packed, condensed fibres (see Fig. 4).

Within the nucleoli a wide variety of structures was seen, depending on cell type and activity. In the quiescent centre, the nucleolus was extremely small, often virtually invisible by DAPI staining. In these nuclei, very little labelling was seen, apart from the 4 very large and bright condensed knobs. This is consistent with the majority of the rDNA being condensed and transcriptionally inactive. An example of a quiescent centre nucleus is shown in Fig. 5.

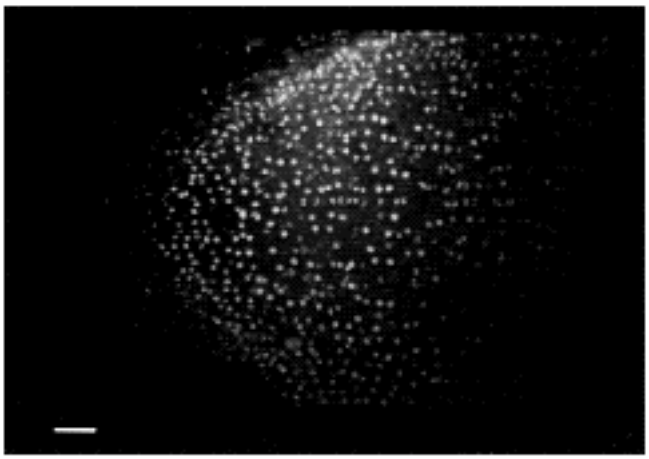

Fig. 3. Low magnification image of a root tip slice. A series of 23 confocal sections, spaced 4 μm apart (i.e. covering a total depth of field of approximately 90 μm), was collected with a 16× objective. The entire data set has been projected for this picture. Each bright spot is a single nucleolus. The labelling is very specific, and extends throughout the tissue so that all types of cell within the tissue are available for high-resolution data collection. Bar, 50 μm.

In the most active meristematic regions the nucleoli were very large, with extensive intranucleolar structure, and the perinucleolar knobs were comparatively small. Although there was a range of internal structures visible, virtually all could be described as being close to one of three types: firstly, in the body of most nucleoli many (10-50) bright foci or spots were observable. The intensity of labelling in these spots was somewhat less than the perinucleolar knobs, suggesting an intermediate degree of condensation. (We have called this first type of nucleolus

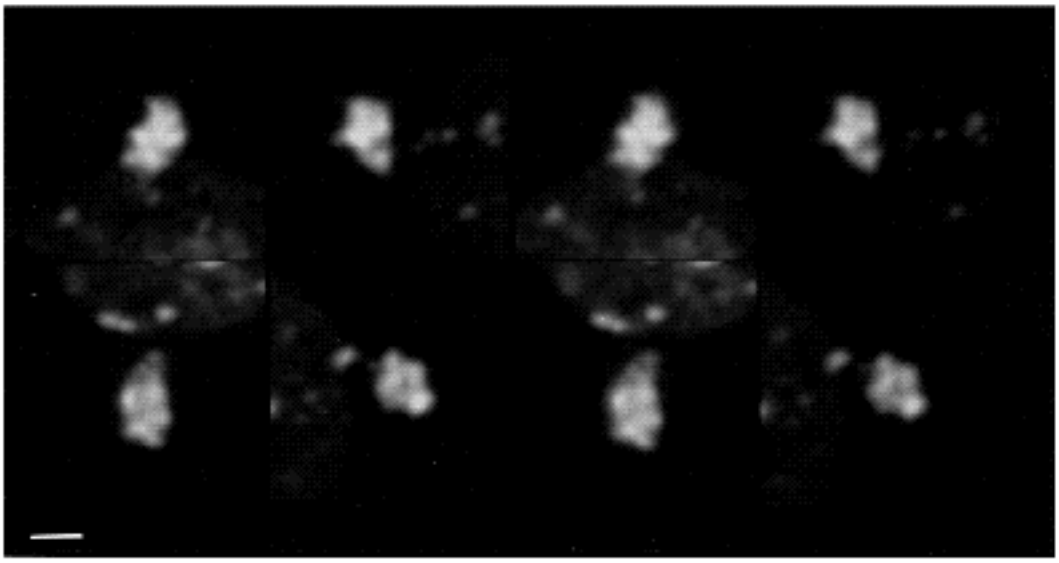

Fig. 4. Detail of the substructure of the perinucleolar knobs (deconvoluted confocal data). In most of the subsequent images the brightness and contrast have been set to optimize the visibility of the nucleolar substructure, and the detail within the bright knobs is lost. Here, stereo pairs of four different perinucleolar knobs are shown. There is generally substructure consistent with condensed, tightly intertwined chromatin fibres. The knobs are either directly situated on the nucleolar periphery, or connected by one or more fine strands. Bar, 1 μm.

'SPOT'.) The spots were continuous with an extensive, fibrous network of weaker labelling (see Fig. 6), which, together with the bright foci, extended throughout the nucleolus. The fibres were particularly apparent in slices at the surface of the nucleolus (Fig. 6A). Secondly, in a proportion of nucleoli a single, large mass of labelling was seen near the centre, in addition to bright spots. (We have called this type 'CM', for central mass.) The central mass comprised several (partially) condensed strands running closely together (see Fig. 7). Again, the labelling intensity was not as great as in the perinucleolar knobs, and so the degree of condensation of the rDNA here was probably not as great. Fainter, presumably less condensed strands, could be seen emanating from the central mass. In some nucleoli, the central mass was very large - up to approximately one third the diameter of the nucleolus, as in Fig. 7. In others it was much smaller, although still clearly identifiable and considerably larger than the other bright foci. (These nucleoli were subcategorized as 'SCM', for small central mass.) The third identifiable arrangement of intranucleolar labelling was characterized by a much more uniform distribution (categorized as 'UNI' nucleoli) and very few or even no bright internal foci. The fainter, fibrous labelling often appeared to be distributed in a characteristic pattern, with darker regions surrounded by brighter labelling. In some cases there were concentric rings of labelling around the centre of the nucleolus and around the nucleolar periphery, interconnected by sheets

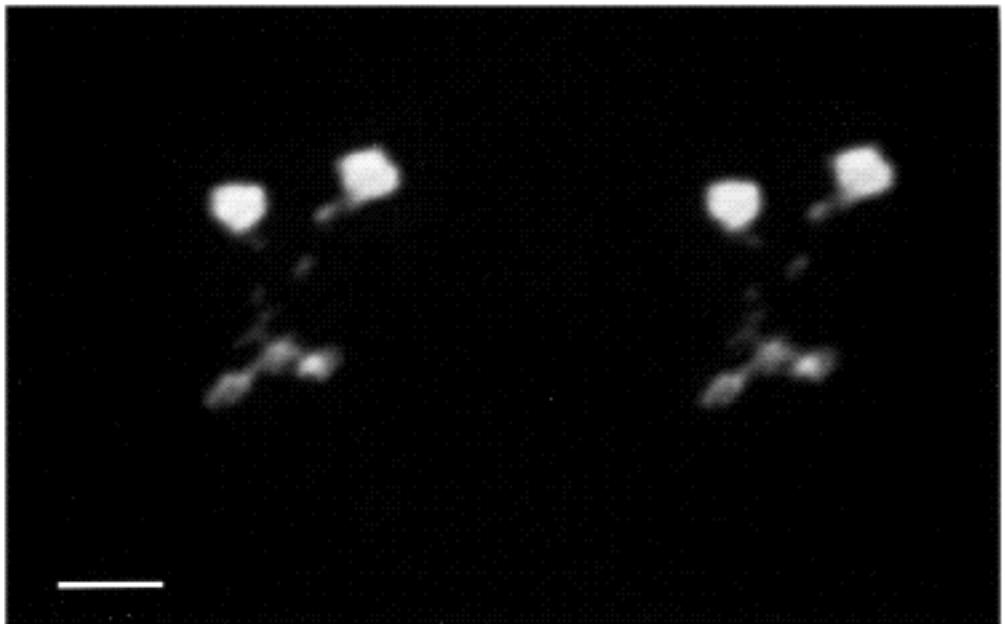

Fig. 5. Stereo pair of labelling in a quiescent centre cell (deconvoluted confocal data). Almost all the labelling is seen in four condensed masses. Data collected at 0.25 μm section spacing. Bar, 2 μm.

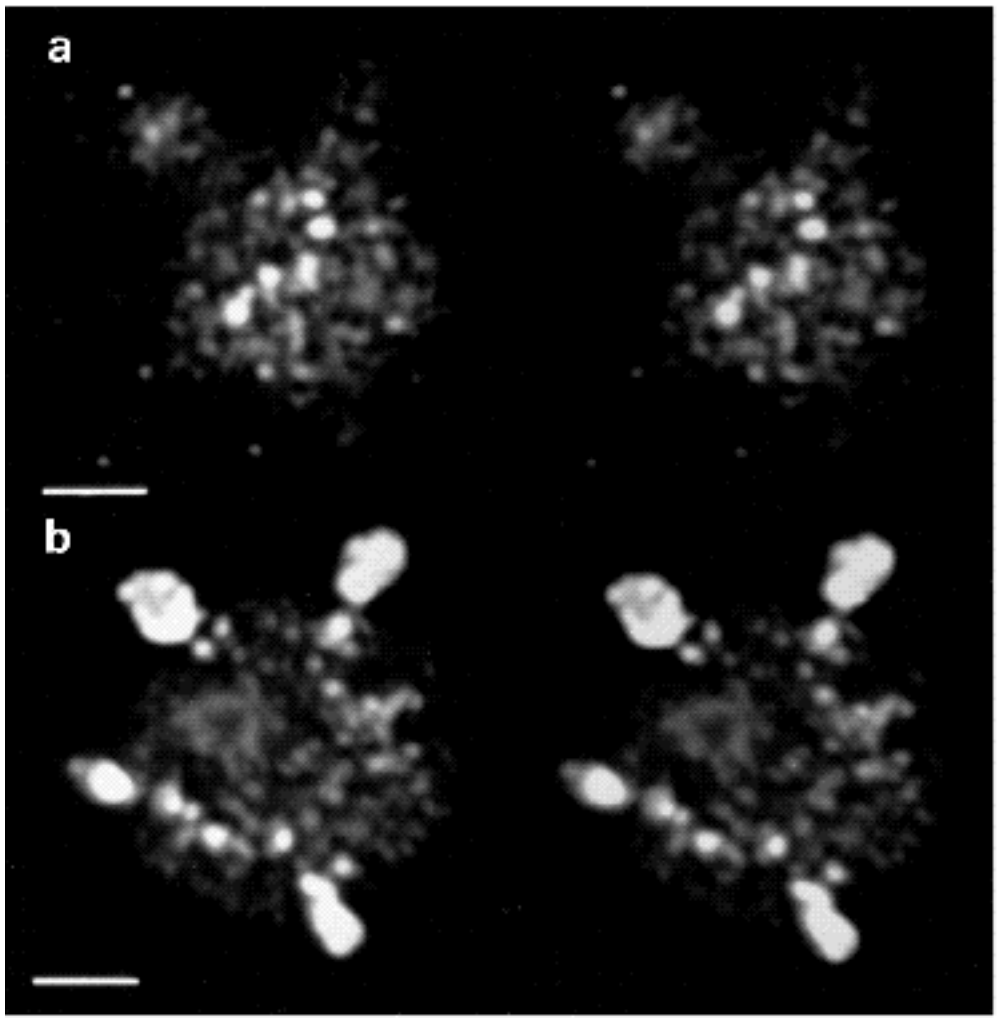

Fig. 6. Stereo pairs of the labelling in a SPOT meristematic cell nucleolus (deconvoluted confocal data). Stereo projections of two slices, each consisting of 5 optical sections 0.25 μm apart, are shown. (a) Slice from the top of the nucleolus. (b) Slice from the centre of the nucleolus. In this nucleolus the four perinucleolar knobs lie, fortuitously, near the central section, and are thus all visible. Within the nucleolus, bright foci, and many more faintly labelled structures are interconnected in an exensive network. Bar, 2 μm.

of labelling. The overall appearance was a cage-like structure as in the example shown in Fig. 8.

In cells at later stages of differentiation, such as those of the root cap, vascular tissue and epidermis, when rDNA transcription is likely to be much lower, the nucleoli were smaller than in the meristematic regions, although larger

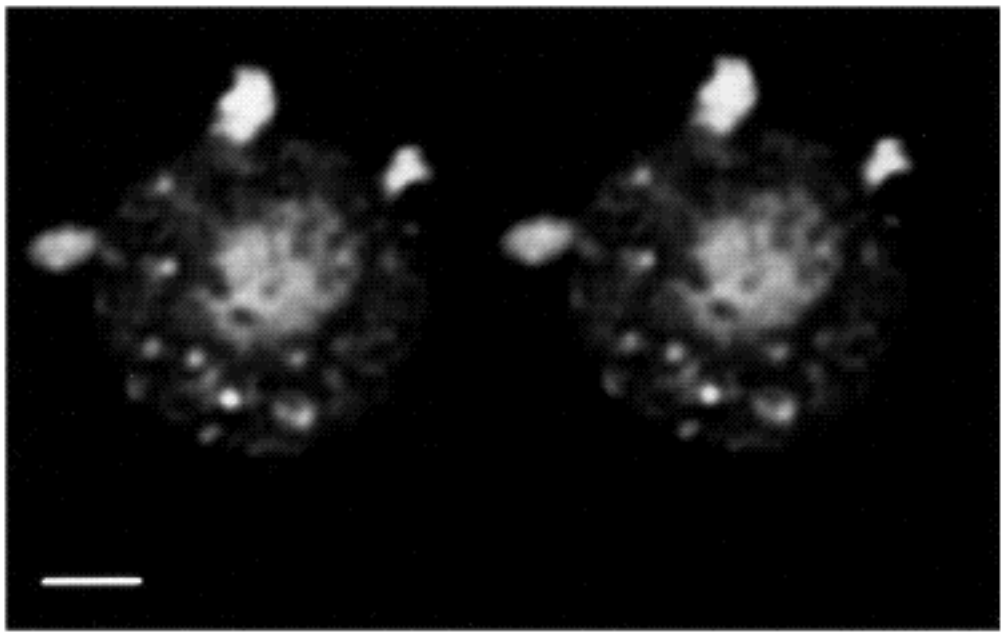

Fig. 7. Stereo pair of central slice projection, calculated from 5 optical sections 0.25 μm apart, from a CM (central mass) nucleolus in the meristematic region (deconvoluted confocal data). The central mass is seen to comprise several partially condensed chromatin fibres clustered together. Finer fibres emanate from the central mass, into a more extensive network, which includes bright foci. Bar, 2 μm.

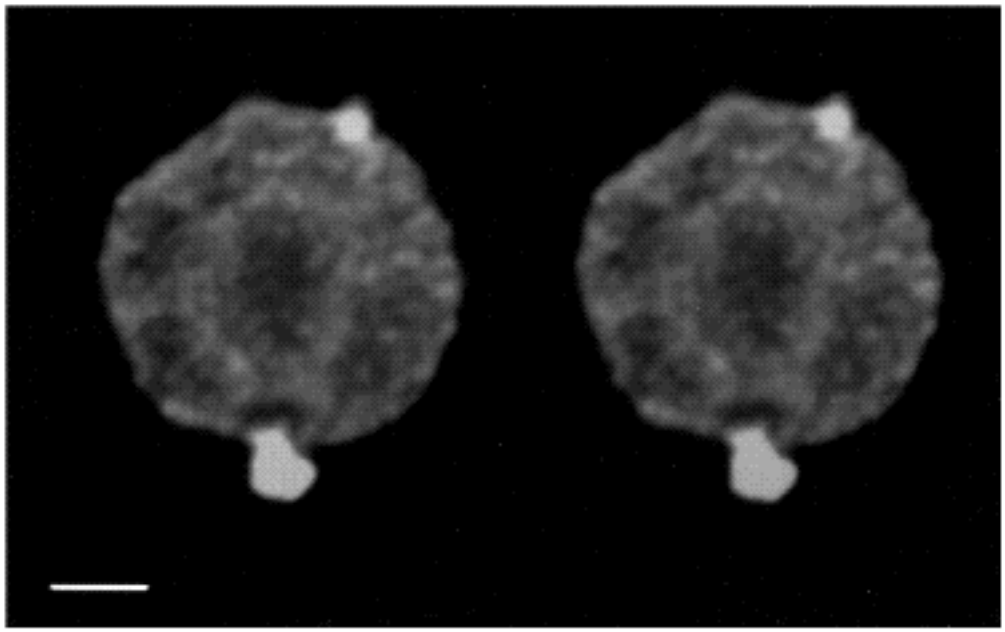

Fig. 8. Stereo pair of central slice projection, calculated from 5 optical sections 0.25 μm apart, from a UNI (uniform) nucleolus in the meristematic region (deconvoluted confocal data). An extended, decondensed fibrous network is seen. Sometimes a few brighter foci are seen, but often, as in this case, there is only the more faintly labelled chromatin. Bar, 2 μm.

than in the quiescent centre. The perinucleolar knobs were large and bright, and nearly all the intranucleolar labelling was contained within a few bright internal masses. An example of a root cap cell nucleolus is shown in Fig. 9.

Quantitation of images

We wished to determine whether the total integrated intensity from in situ labelling of a nucleolus was a good measure of the amount of rDNA, which would be expected to vary by a factor of 2 between G_1 and G_2 in the cell cycle. Previous studies have shown that measurements of integrated fluorescence intensity of DAPI give a good measure of DNA content (Corke et al., 1987), and we therefore measured the integrated fluorescence intensity both of rDNA by FITC fluorescence and of total DNA by DAPI fluorescence for each of a number of different cells in several different tissue slices. The images were measured using wide-field optics and a cooled CCD camera, both because our confocal microscope cannot image DAPI and because total integrated fluorescence intensity can be measured by integrating in a single wide-field focal section, thus simplifying the measurement of large numbers of cells. Nineteen fields of view were randomly selected and measurements of DAPI and FITC integrated intensity were made for each of the nuclei (between 2 and 18 per field). Only entire, undamaged nuclei were included in the measurements. Where an unambiguous assignment of nucleolar labelling type could be made at this low magnification, this was noted. Otherwise the nucleolus was designated 'ND' for not determined. A plot of DAPI versus FITC intensity values is shown in Fig. 10. Taking the data as a whole there is a high positive correlation between total DNA (DAPI) and total rDNA (FITC)

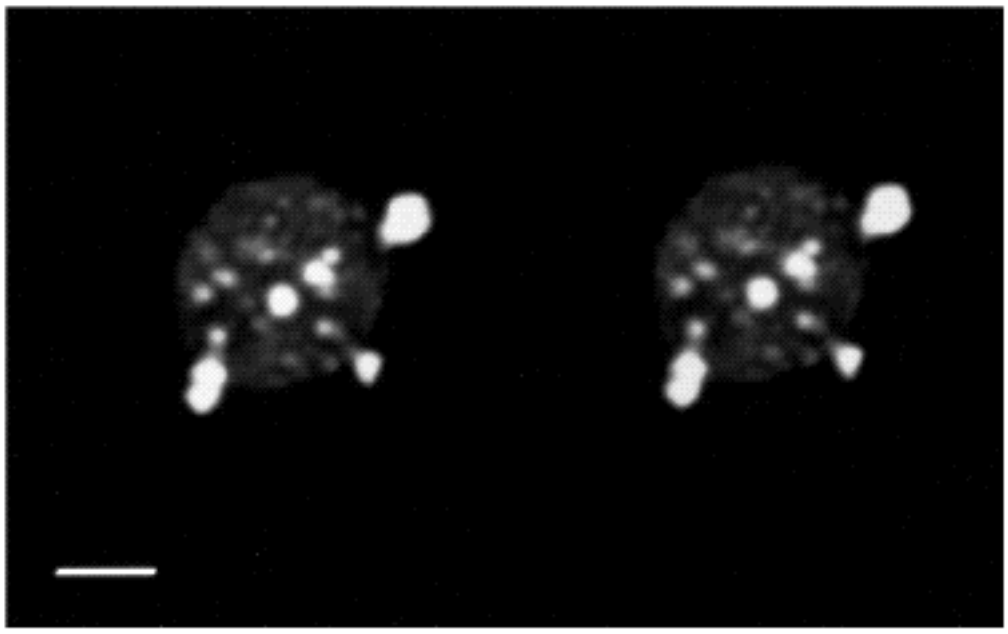

Fig. 9. Stereo pair of central slice projection, calculated from 5 optical sections, 0.25 μm apart, from a root cap nucleolus, typical of the structure seen in more differentiated, and less-active cell types (deconvoluted confocal data). Most of the internal chromatin is condensed into bright structures, and the amount of extended, more faintly labelled chromatin is much less than in the meristematic nucleoli. Bar, 2 μm.

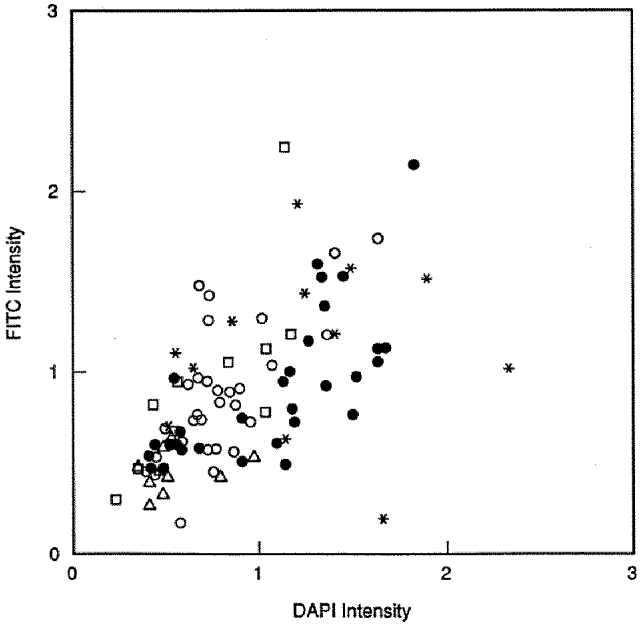

Fig. 10. A graph of integrated in situ fluorescence intensity (rDNA) against integrated DAPI intensity (total DNA), showing a clear correlation between rDNA and total DNA, within the range expected from cell cycle differences, and irrespective of nucleolar type. Key: ○, SPOT; *, UNI; □, CM; △, vascular tissue; ●, type not determined.

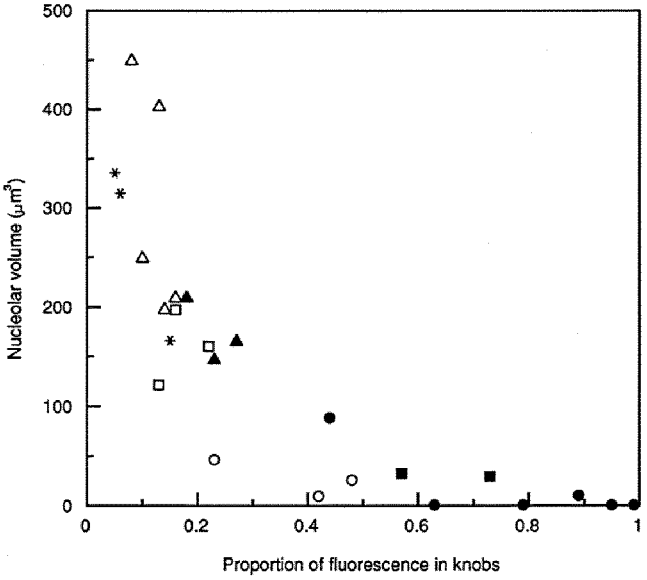

Fig. 11. A graph of proportion of rDNA labelling localized to the perinucleolar knobs, plotted against nucleolar volume. There is an obvious negative correlation, showing that as the nucleolus becomes more active, rDNA from the perinucleolar knobs decondenses causing an increase in nucleolar volume. Key: □, SPOT; △, UNI; *, CM; ▲, SCM; ○, root cap; ■, epidermis; ●, quiescent centre.

values. As Fig. 10 shows, this correlation holds irrespective of nucleolar type. To test the distribution statistically, a non-parametric test of correlation (Spearman's rank correlation test) was used. The pooled data, which had a sample size of 93, gave a very significant correlation ($P < 0.01$; $r_S = 0.657$) (Sokal and Rohlf, 1981). Thus we conclude that, assuming the DAPI fluorescence intensity is a good measure of total DNA content, the rDNA in situ fluorescence intensity can be used as a measure of rDNA content, and is not dependent on the degree of condensation of the rDNA in particular nucleoli. The variation in both total DNA and rDNA content measured in this way is in the expected range for cell cycle differences.

Having established that integrated fluorescence intensity could be used as a quantitative measure of rDNA, we next determined whether the amount of condensed perinucleolar rDNA was related to nucleolar activity. For this, we measured the total integrated in situ fluorescence, in this case by integrating all the relevant sections from confocal data stacks of individual nuclei. Since the section spacing was substantially less than the confocal depth of field, this integration should give a reliable measure of the specimen integrated fluorescence. We also measured the integrated fluorescence intensity of each of the perinucleolar knobs, and expressed this as a fraction of the total rDNA fluorescence for each nucleolus. Finally, we also estimated the nucleolar volume by measuring the radius of the body of the nucleolus. Since these nucleoli are spherical to a good approximation this can be used to give an estimate of the nucleolar volume. The fraction of total intensity present in the perinucleolar knobs is shown plotted as a function of nucleolar volume in Fig. 11. The data show a negative correlation between nucleolar volume and amount of perinucleolar rDNA and, in addition, that different populations of cell types occupy different (but overlapping) areas of this graph. Taking the data as a whole, a Spearman's rank correlation coefficient $r_S = -0.908$ was obtained with a total sample size of 25. This indicates a very highly significant ($P \ll 0.01$) negative correlation between perinucleolar rDNA and nucleolar volume. It was not possible to test for significance of differences between individual cell populations due to the small number of nuclei measured in each cell type. Nevertheless, striking differences between these cell types are apparent from Fig. 11. The data points are plotted exactly as determined. However, some corrections in the data points could be argued for. The CM nucleoli have a considerable amount of internal, bright labelling in the central mass and this integrated intensity could be added to the perinucleolar knob intensity to give the proportion of condensed rDNA. This would place the CM nucleoli much closer to the main cluster centred along the diagonal, and would suggest an even stronger negative correlation between nucleolar volume and amount of condensed rDNA. The same argument would apply to the highly differentiated root cap and epidermal cell nucleoli, which have a few large internal masses of condensed rDNA.

DISCUSSION

We have demonstrated that rDNA in the nucleoli of different cells from the apices of *Pisum sativum* seedling roots shows several different and characteristic patterns of distribution. This is very likely to reflect the different cellular metabolic activities and requirements for ribosome synthe-

sis in the different cells within the root tips. Our results suggest at least three different levels of rDNA condensation, as judged by relative intensity of in situ labelling. The most condensed rDNA is seen in the perinucleolar knobs. Within the nucleoli we observe large central masses of rDNA and smaller foci, which, although bright, are proportionately less bright than the knobs. In addition to the more condensed regions of rDNA, we have also shown the presence of various amounts of more faintly labelled, decondensed rDNA. In some of the most active (UNI) nucleoli all the internal labelling is of this latter type.

We suggested previously (Rawlins and Shaw, 1990) that the nucleolus-associated chromatin in the perinucleolar knobs decondensed as the nucleolus became more active. In this paper we have used quantification of both wide-field and confocal images to estimate the amount of rDNA from the integrated in situ fluorescence. This analysis has shown that the smaller the proportion of the total rDNA fluorescence contained in the perinucleolar knobs the larger the nucleolar volume. This is seen most dramatically in the progression from the almost completely inactive quiescent centre nucleoli to the very active meristematic nucleoli, the proportion of rDNA in the knobs varying from almost all to almost none. Many studies (see, e.g., Hadjiolov, 1985; Miller and Brown, 1969; Miller and Knowland, 1970) have shown that nucleolar volume is correlated with nucleolar activity. Thus our results show that as the requirement for ribosome biosynthesis, and rDNA transcription, increases, more copies of the rDNA contained in the perinucleolar knobs decondense, resulting in an increase in size of the nucleolus. Taking all the different arrangements and cell types observed, the clear conclusion is that the lower the presumed transcriptional activity, the greater the proportion of rDNA fluorescence contained within the various brightly staining structures, either outside the nucleolus in the knobs or inside in bright foci or larger masses. The simplest conclusion would be that the most decondensed, faintest labelled rDNA represents the transcriptionally active genes. However, we have no means of knowing what proportion of this decondensed rDNA is active even in the largest (UNI) nucleoli - merely that nearly all the rDNA is decondensed within the body of the nucleolus.

An obvious question is the relation between the in situ labelling we have visualized and the ultrastructure revealed by thin-section electron microscopy. Previous work (e.g. see Nougarede et al., 1990) has shown that pea tissue has a fairly standard nucleolar structure, including fibrillar centres, dense fibrillar material and granular component. A large central fibrillar centre has been seen in some dormant cotyledonary bud cells, thought to be arrested in $G_{0\text{-}1}$ (Nougarede et al., 1990); in other cells many considerably smaller (approximately 0.2-1.0μm in diameter) fibrillar centres are seen. The large central masses of fairly condensed rDNA we have seen may correspond to the large central fibrillar centres. However, we have not found any correlation of nucleoli with a central mass (CM) with position in the cell cycle; CM nucleoli have been found with DAPI staining, which must correspond to both G_1 and G_2 (results not shown). Nougarede et al. (1990) also showed, by DNase-gold labelling, the presence of DNA in the fibrillar centres, but also elsewhere in the nucleolus. In view of their size and distribution, the spots or foci we have observed in many nucleoli may correspond to fibrillar centres. We cannot, however, prove this definitively without directly comparing fluorescence in situ labelling with electron microscope images of the same nucleoli. In any case, the labelling we have observed is too extensive to be ascribed solely to fibrillar centres. It is quite consistent with the widely dispersed DNA we have demonstrated by DAPI labelling within the nucleoli of *Spirogyra* and human MRC5 culture cells (Jordan et al., 1992). It is interesting to note that Knibiehler et al. (1982) have shown that the nucleoli in an established *Drosophila* cell line lacked fibrillar centres, thus providing evidence that conventional fibrillar centre structures are not obligatory for transcriptional activity.

Whether the foci represent fibrillar centres or not, our data suggest that such foci are not necessary for transcription, since some of the largest and most transcriptionally active nucleoli, the UNI nucleoli, completely lack foci. (It should be noted that the total integrated intensity of the rDNA labelling is approximately the same in the UNI nucleolar and the other types.) Recently, Leitch et al. (1992) have also suggested that condensed foci of rDNA are not necessary for transcription in rye. The detailed arrangement of the labelling in the UNI nucleoli is interesting. In some cases there is a central darker region, in others a more regular structure with several darker areas and sheets of labelling between is apparent. This general pattern of labelling is reminiscent of the immunofluorescence labelling visualized by Corben et al. (1989) using a monoclonal antibody to a nucleolar matrix protein in carrot suspension cell nucleoli. It is possible that this labelling pattern represents an underlying nucleolar matrix on which the most decondensed rDNA is arranged.

Daneholt and colleagues have obtained detailed electron micrographs of transcription complexes from the Balbiani ring BR2 transcription complexes in *Chironomus tentans* salivary gland polytene nuclei (Andersson et al., 1980; Lamb and Daneholt, 1979). Although many details of the latter transcription must differ significantly from rDNA transcription - the transcript in BR2 is much larger, and a different RNA polymerase is involved - the general geometrical principles may make a comparison useful. In the BR2 transcription, a single transcription unit is about 7.7 μm in length in situ, and the unit together with its multiple nascent transcripts is approximately 0.1-0.2 μm in diameter (Andersson et al., 1980). Surprisingly, this is only 2-3 times more condensed than the familiar Miller spreads of 'Christmas trees'(Lamb and Daneholt, 1979; Miller, 1981). Since the BR2 75S transcript is about 36 kb in length (i.e. about 6 times the length of the rDNA primary transcript), we might expect a single, maximally active rDNA repeat to be a little over 1 μm in length in situ, and rather less than the diameter of the BR2 transcription units. This would be quite consistent with the extended fibrous structures corresponding to dispersed intranucleolar rDNA that we have shown. A typical large pea nucleolus, 200 μm^3 in volume, could accommodate approximately 25,000 such units if they were packed to fill the entire volume. Thus, given that there are about 4000 copies of the rDNA in pea (Ellis et al., 1984), there would be no problem accommodating them all, at least within the observed labelled

volume of the UNI nucleoli, at this level of decondensation. We have shown that, in UNI nucleoli, nearly all the rDNA contained in the perinucleolar knobs has at least partially decondensed into the body of the nucleolus, but we cannot determine what proportion of these copies are actually transcriptionally active. It is certainly possible that most of the rDNA copies could be active in at least some of the meristematic nucleoli. However, in view of the fact that some plant cells have an order of magnitude more rDNA than animal cells, and that closely related species or varieties can exhibit large differences in amounts of rDNA without any apparent phenotypic consequences (e.g. see Thompson and Flavell, 1988, and references therein), it seems most likely that a large proportion of the rDNA copies are transcriptionally inactive. It is likely that the detailed conformation of the rDNA is complex and dynamic, and many studies of chromatin have suggested a number of different levels of organization. The results we have presented show the larger-scale levels of nucleolar organization of rDNA and the structural changes consequent on changes in regulation of the expression of these genes.

This work was supported by the Agricultural and Food Research Council of the UK via a grant-in-aid to the John Innes Institute, and a project grant from the Plant Molecular Biology initiative. M.I.H. was supported by a John Innes Foundation studentship. We thank Gwyn Jordan for helpful advice and discussion. We thank David Agard and John Sedat for sharing computer programs with us.

REFERENCES

Agard, D. A., Hiraoka, Y., Shaw, P. and Sedat, J. W. (1989). Fluorescence microscopy in three dimensions. *Meth. Cell Biol.* **30**, 353-377.

Andersson, K., Bjorkroth, B. and Daneholt, B. (1980). The in situ structure of the active 75 S RNA genes in Balbiani rings of *Chironomus tentans. Exp. Cell Res.* **130**, 313-326.

Corben, E., Butcher, G., Hutchings, A., Wells, B. and Roberts, K. (1989). A nucleolar matrix protein from carrot cells identified by a monoclonal antibody. *Eur. J. Cell Biol.* **50**, 353-359.

Corke, F. M. K., Hedley, C. L., Shaw, P. J. and Wang, T. L. (1987). An analysis of seed development in *Pisum sativum.* V. Fluorescence triple staining for investigating cotyledon cell development. *Protoplasma* **140**, 164-172.

Cox, K. H., DeLeon, D. V., Angerer, L. M. and Angerer, R. C. (1984). Detection of mRNAs in sea urchin embryos by *in situ* hybridization using asymmetric RNA probes. *Dev. Biol.* **101**, 485-502.

Deltour, R. and Mosen, H. (1987). Proposals for the macromolecular organization of the higher plant nucleonema. *Biol. Cell.* **60**, 75-86.

Ellis, T. H. N., Davies, D. R., Castleton, J. A. and Bedford, I. D. (1984). The organization and genetics of rDNA length variants in peas. *Chromosoma* **91**, 74-81.

Geuskens, M. and Bernhard, W. (1966). Cytochemie ultrastructure nucleole. *Exp. Cell Res.* **44**, 579-598.

Goessens, G. (1984). Nucleolar structure. *Int. Rev. Cytol.* **87**, 107-158.

Goessens, G. (1976). High resolution autoradiographic studies of Ehrlich tumor cell nucleoli. *Exp. Cell Res.* **100**, 88-94.

Hadjiolov, A. A. (1985). *The Nucleolus and Ribosome Biogenesis.* Cell Biol. Monogr. 12. Springer Verlag, Wien, New York.

Hernandez-Verdun, D. and Bouteille, M. (1979). Nucleologenesis in chick erythrocyte nucleoli reactivated by cell fusion. *J. Ultrastruct. Res.* **69**, 164-179.

Jordan, E. G. (1984). Nucleolar nomenclature. *J. Cell Sci.* **67**, 217-220.

Jordan, E. G. (1991). Interpreting nucleolar structure: where are the transcribing genes? *J. Cell Sci.* **98**, 437-442.

Jordan, E. G., Zatsepina, O. V. and Shaw, P. J. (1992). Widely dispersed DNA within plant and animal nucleoli visualised by 3-D fluorescence microscopy. *Chromosoma* **101**, 478-482.

Knibiehler, B., Mirre, C. and Rosset, R. (1982). Nucleolar organizer structure and activity in a nucleolus without fibrillar centres: the nucleolus in an established *Drosophila* cell line. *J. Cell Sci.* **57**, 351-364.

Lamb, M. M. and Daneholt, B. (1979). Characterization of active transcription units in Balbiani rings of *Chironomus tentans. Cell* **17**, 835-848.

Leitch, A.R. Mosgoller, W., Shi, M. and Heslop-Harrison, J. S. (1992). Different patterns of rDNA organization at interphase in nuclei of wheat and rye. *J. Cell Sci.* **101**, 751-757.

Martin, M., Moreno Diaz de la Espina, S. and Medina, F. J. (1989). Immunolocalization of DNA at nucleolar structural components in onion cells. *Chromosoma* **98**, 368-377.

Medina, F. J. (1989). Meeting report: the nucleolus in the spotlight. *Eur. J. Cell Biol.* **50**, 244-246.

Miller, L. and Brown, D. D. (1969). Variation in the activity of nucleolus organisers and their ribosomal gene content. *Chromosoma* **28**, 430-444.

Miller, L. and Knowland, J. (1970). Reduction of ribosomal RNA synthesis and ribosomal RNA genes in a mutant of *Xenopus laevis* which organises only a partial nucleolus. II. The number of ribosomal RNA genes in animals of different nucleolar types. *J. Mol. Biol.* **53**, 329-338.

Miller, O. L. (1981). The nucleolus, chromosomes and visualization of gene activity. *J. Cell Biol.* **91**, 15s-27s.

Mirre, C. and Stahl, A. (1978). Peripheral RNA synthesis of fibrillar centre in nucleoli of Japanese quail oocytes and somatic cells. *J. Ultrastruct. Res.* **64**, 377-387.

Nougarede, A., Landre, P. and Jennane, A. (1990). Intranucleolar visualization of nucleic acids and acidic proteins in inhibited and rectivated pea cotyledonary buds. *Protoplasma* **156**, 183-191.

Rawlins, D. J. and Shaw, P. J. (1990). Three-dimensional organization of ribosomal DNA in interphase nuclei of *Pisum sativum* by in situ hybridization and optical tomography. *Chromosoma* **99**, 143-151.

Sambrook, J., Fritsch, E. F. and Maniatis, T. (1989) *Molecular Cloning,* 2nd edn. Cold Spring Harbor Laboratory Press, NY.

Scheer, U. and Rose, K. (1984). Localization of RNA polymerase I in interphase cells and mitotic chromosomes by light and electron microscopic immuno-cytochemistry. *Proc. Nat. Acad. Sci. USA* **81**, 1431-1435.

Schwarzacher, H. G. and Wachtler, F. (1991). The functional significance of nucleolar structures. *Ann. Genet.* **34**, 151-160.

Shaw, P. J. and Rawlins, D. J. (1991a). The point spread function of a confocal microscope: its measurement and use in deconvolution of 3-D data. *J. Microsc.* **163**, 151-165.

Shaw, P. J. and Rawlins, D. J. (1991b). Three-dimensional fluorescence microscopy. *Prog. Biophys. Mol. Biol.* **56**, 187-213.

Sokal, R. R. and Rohlf, F. J. (1981). *Biometry*, 2nd edn, p. 607, Freeman and Co., San Francisco

Stahl, A. (1982). Nucleolus and nucleolar chromosomes. In: *The Nucleolus* (ed. E. G. Jordan and C. A. Cullis), *S.E.B. Seminar Series 15*, pp. 1-24, Cambridge University Press, Cambridge.

Thiry, M., Scheer, U. and Goessens, G. (1988a). Localization of DNA within Ehrlich tumor cell nucleoli by immuno-electron microscopy. *Biol. Cell* **63**, 27-34.

Thiry, M., Scheer, U. and Goessens G. (1988b). Immuno-electron microscopic study of DNA during mitosis in Ehrlich tumor cells. *Eur. J. Cell Biol.* **47**, 346-357.

Thompson, W. F. and Flavell, R. B. (1988). DNase I sensitivity of ribosomal RNA genes in chromatin and nucleolar dominance in wheat. *J. Mol. Biol.* **204**, 535-548.

Traas, J. A., Beven, A. F., Doonan, J. H., Cordewener, J. and Shaw, P. J. (1992). Cell-cycle-dependent changes in labelling of specific phosphoproteins by the monoclonal antibody MPM-2 in plant cells. *The Plant J.* **2**, 723-732.

Wachtler, F., Hartung, M., Devictor, M., Wiegant, J., Stahl, A. and Scwarzacher, H. G. (1989). Ribosomal DNA is located and transcribed in the dense fibrillar component of human Sertoli cell nucleoli. *Exp. Cell. Res.* **184**, 61-71.

Warner, J. R. (1989). The nucleolus and ribosome formation. *Curr. Opin. Cell Biol.* **2**, 521-527.

(Received 17 September 1992 - Accepted 24 November 1992)